Indian Journal of Chemical Technology
Vol. 30, November 2023, pp. 848-862
DOI: 10.56042/ijct.v30i6.6551

A study on entropy generation of hydromagnetic oscillating flow of a diamond-ethylene glycol+water based couple stress nanofluid in a vertical channel in the presence of Joule heating and thermal radiation

A Subramanyam Reddy[1] & S Rajamani[1,2]*

[1]Department of Mathematics, School of Advanced Sciences, Vellore Institute of Technology, Vellore-632014, Tamil Nadu, India

[2]Department of Mathematics, Einstein College of Arts and Science, Seethaparpanallur, Tirunelveli-627012, Tamil Nadu, India

*E-mail: sraja199317@gmail.com

The current work communicates the entropy generation analysis of oscillating flow of magnetohydrodynamic couple stress nanofluid in a vertical channel. The main objective of present study is to examine the entropy analysis of a magnetohydrodynamic couple stress nanofluid. In this study, water and ethylene glycol (50:50) and diamond are used as the base fluid and nanoparticles, respectively. The effects of radiative heat, Ohmic, and viscous dissipation are all considered. By employing the perturbation process, the governing partial differential equations are transformed into the set of ordinary differential equations, which are then deciphered by implementing the Runge-Kutta fourth-order scheme with shooting technique. The obtained outcomes reveal that, amplifying viscous dissipation promising the temperature whereas the reverse is true for the influence of couple stress viscosity and Hartmann number. Heat transfer rate is decelerating with the boost up in Hartmann number at the walls while it is accelerating with the increment in viscous dissipation at the right wall. Entropy is escalating for intensifying viscous dissipation, and thermal radiation whereas the reverse is true for the impression of couple stress viscosity, and volume fraction of nanoparticles. Bejan number is falling for escalating volume fraction of nanoparticles, and viscous dissipation while it is enhancing with escalation in couple stress parameter.

Keywords: Bejan number, Couple stress nanofluid, Entropy generation, Joule heating, Oscillating flow, Thermal radiation

The field of nanofluids has received intense attention since the mid-20th century. Many engineering applications involve nanofluids, such as the radiators in automation, biomedicines, solar energy, nuclear energy, micro-nano scale electronics, and space vehicles[1-11]. Basha *et al.*[12] made a numerical attempt to study the hydromagnetic flow of diamond-ethylene glycol and water mixture nanofluid on three different geometries with the support of Runge-Kutta Fehlberg process. Here the authors claimed that the concerned study is dedicated for the application of solar energy. Hosseinzadeh *et al.*[13] examined the magneto-hydrodynamic flow of the combination of ethylene glycol and water with the fusion of multiwall carbon nanotubes and silver nanoparticles through a permeable medium by adopting the Runge-Kutta fifth order technique. The impressions of thermal radiative heat flux, shape factor of nanoparticles, and viscous dissipation have analysed by the authors. Massoudi and Hamida[14] numerically studied the diamond-water nanofluid flow past inside a trapezoidal cavity surrounded by an elliptical baffle with the consideration of thermal radiation, heat generation/sink, and Lorentz forces effect by adopting the finite element process. Saleh and Sundar[15] experimentally inspected the exergy efficiency and the irreversibility analysis on the fusion of diamond and magnetite nanoparticles with the combination of water and ethylene glycol through a circular tube. Muneeshwaran *et al.*[16] made a survey to inspect the upcoming development of nanofluid on heat transmission occurrence with the appeal that the thermal conductivity of the nanoparticles is boosting the heat transmission and the stability of the fusion of nanoparticles can be influenced by thermophysical characteristics.

Despite its significance, non-Newtonian fluids remain an area of research in engineering that is still developing. Engineering applications typically involve these fluids such as polymer extrusion, crystallization of liquids, and bio fluids. One of the noteworthy non-Newtonian models is couple stress model is related to various science and engineering utilization like lubricants, dissolvent, and synovial fluids[17-21]. Lubricants are often modelled mathematically as couple stress fluids due to the effect additives have on their rheological characteristics. Based on the root of continuum

concept, Stokes[22] proposed a couple stress theory to model the mechanical interactions between fluid particles. The author studied the flow behaviour of electrically conducting couple stress fluid on hydromagnetic field. Adesanya and Makinde[23] investigated the impression of couple stresses on incompressible viscous fluid via permeable channel with the consideration of entropy generation, and Bejan number analysis by adopting the modified Adomian decomposition method. Ramesh *et al*.[24] numerically explored the hydromagnetic nanofluid flow with couple stress through a perpendicular permeable strait with the impressions of heat generation/absorption, thermophoresis, and radiative thermal flux by using the Runge-Kutta scheme. Dhlamini *et al*.[25] proposed the innovative numerical model to the couple stress fluid based on the impact of thermal conductivity and viscosity with the support of spectral quasi-linearization method. Umavathi and Beg[26] studied the nanofluid flow with couple stresses through a porous passage with the analysis of couple stress parameter's influence on stationary and oscillatory convection by using the perturbation and Runge-Kutta-Gill quadrature scheme, respectively. Here the authors believed that the concerned study is significant in the field of petroleum recovery. Usman *et al*.[27] analytically examined the magnetohydrodynamic nanofluid flow with couple stress and the suspension of the fusion of single and multiwall carbon nanotubes past an unsteady rotating disc by incorporating the homotopy analysis process. Rajamani and Reddy[28] inspected the hydromagnetic pulsating nanofluid flow with couple stress between a pair of parallel walls with the account of radiative thermal flux and Ohmic heating by means of the perturbation procedure. Recently, Jawad *et al*.[29] studied the nanofluid flow with couple stress on a penetrable surface with radiative thermal flux, heat generation, thermophoresis, Brownian motion, and magnetic field impressions for the improvement of drug targeting related bio industrial nanodevices applications.

A flow with rhythmic and intermittent variations is termed as pulsatile flow. In view of vast industrial, engineering, and science applications like mechanical heart, dynamics of blood in cardiovascular system, medical processes with pressure gradient, and development of coastal area dominated by waves[30-34] there is lot to investigate about the flow with periodic variations induced by the pressure gradient. Zamzari *et al*.[35] numerically deliberated the heat transfer rate and irreversibility analysis of pulsating flow through a channel with the aid of the finite volume procedure. Srinivas *et al*.[36] scrutinized the hydromagnetic nanofluid with pulsation via permeable strait with the impression of viscous dissipation, Ohmic heating, and radiative thermal flux by using the perturbation method. Shawky[37] analyzed the heat transfer rate on hydromagnetic pulsating dusty fluid flow with Ohmic dissipation by adopting perturbation process with Lightill procedure. Ahmed and Xu[38] analytically scrutinized the impression of radiative thermal flux, and magnetic parameter on pressure driven nanofluid flow through a microchannel. Ye *et al*.[39] outlined that the inspection on pulsatile flow is noteworthy in microelectronic engineering, industrial, biomedical engineering, and biochemical engineering. Venkatesan and Reddy[40] discussed the hydromagnetic pulsating flow of Oldroyd-B nanoliquid *via* strait with the impressions of radiative thermal flux, viscous and Ohmic dissipations by means of the perturbation procedure.

Entropy analysis demonstrates the level of vitality, which is inaccessible and the ratio of the irretrievable energy of the system. Analysing the entropy generation helps to improve the thermal enactment of the system. Entropy is clearly significant thing to make the efficient energy system due to its episodes in air coolers, atomic power, chillers, and solar power. Bejan[41] showed an exceptional investigation on entropy analysis for temperature gradient and frictional impacts in detail. Here the author has shown the specified values for the pertinent parameters to signify the entropy generation. Dhahri *et al*.[42] numerically inspected the entropy production of the pulsatile flow in a permeable medium by adopting the finite element method which is based on control volume method. Here the authors investigated the Bejan number for the concerned model. Hosseinzadeh *et al*.[43] analytically studied the entropy generation on the Bodewadt nanofluid flow on a cylindrical outward with the influence of viscous dissipation, and Bejan number analysis by employing the homotopy perturbation method. Upadhya *et al*.[44] inspected the entropy analysis of the Casson, micropolar and hybrid nanoliquid on a curved elongated surface with the impact of Ohmic dissipation and radiative thermal flux with the aid of shooting technique. In view of great significance in the day to day life applications, science, and industry such as glass processing,

malleable layers, power generation, aviation devices, geographical development, polymer extrusion, and dye extruding[45,46] there is a lot to deliberate about thermal radiation subject to Ohmic and viscous dissipations. Kumar *et al*.[47] numerically analyzed the pulsating hydromagnetic Casson fluid flow via vertical permeable strait with the impression of radiative heat, Ohmic heating and frictional effects by utilizing the shooting scheme with fourth-order Runge-Kutta process. Zhao *et al*.[48] inspected the sway of radiative heat on the hydromagnetic stagnation point flow of tangent hyperbolic nanoliquid over an extendable sheet with the study of entropy generation approach. Here the authors utilized the second law of thermodynamics to measure the irreversibility factor. Loganathan *et al*.[49] discussed the impression of thermal radiation on non-Newtonian nanofluid on extendable surface with the entropy analysis.

Inspired by the aforementioned studies, the foremost objective of the current inspection is to analyze the entropy production of magnetohydrodynamic oscillating nanofluid with couple stress between straight up parallel walls. In this analysis, the combination of water and ethylene glycol (50:50) and diamond are chosen to be the base fluid and nanoparticles, respectively. The influences of radiative heat, Ohmic and viscous dissipations are deliberated. The governing partial differential equations are rehabilitated into the set of ordinary differential equations by deploying the perturbation process then deciphered by employing the Runge-Kutta fourth-order scheme with shooting procedure. The present work is significant in the field of nano-drug delivery, biological and complex fluids, drug targeting, solar energy, tissue heat conduction, and biomedicines. It is crucial for maximizing the performance of microfluidic systems used in point-of-care diagnostics, drug screening, and lab-on-a-chip technologies. The heat produced by operating electronic gadgets can cause cooling systems to have pulsating flow conditions. Pulsatile flow can occur in aerospace applications due to the cyclic nature of propulsion systems or flow control devices. The profiles of temperature, velocity, entropy production, and Bejan number for different values of emerging parameters are drawn graphically and discussed in detail. Shear stress distribution and heat transmission rate of couple stress nanoliquid for various emerging parameters are tabulated and explained well. Owing to the importance of this kind of problem, the present analysis aims to manifest answers to the following research questions: (i) What are the impacts of Hartmann number and volume fraction of nanoparticles on velocity distribution of nanofluid? (ii) How do the Grashof number and non-Newtonian parameter affect the velocity of nanofluid? (iii) What is the influence of viscous dissipation and magnetic field onsteady and unsteady temperature distributions of nanofluid? (iv) What is the significance of nanoparticle volume fraction and magnetic fieldon heat transfer rate of couple stress nanofluid?.

Formulation of the problem

In this work, incompressible laminar flow of electrically preserved magnetohydrodynamic nanofluid with couple stress subject to oscillating pressure gradient between a pair of parallel straight up walls is deliberated. The mixture (50:50) of ethylene glycol and water is picked as base fluid (couple stress fluid) and diamond is picked as nanoparticle. The episodes of radiative thermal flux, Ohmic and frictional dissipations are accounted. The schemetic illustration of the present work is revealed in Fig. 1. The x^*-axis matches with the left wall whereas the y^*-axis is perpendicular to the walls. The pulsatile pressure gradient induced the couple stress nanofluid flow along with buoyancy forces in its direction. An intensity B_0 of applied magnetic field is enforced upright to the flow direction. The right and left walls are upholding the temperatures T_1 and T_0 accordingly ($T_0 < T_1$). In the current study, we assume that the walls are infinite in length, so that the flow is essentially axial, so that only x^*-component of u^* of

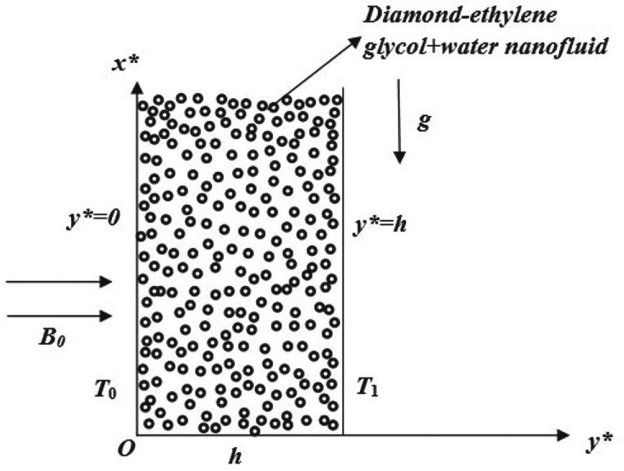

Fig. 1 — Schematic diagram of the current model

the velocity does not vanish. The condition of fully developed flow implies that $\frac{\partial u^*}{\partial x^*}=0$. Since the velocity is solenoidal, we obtain $\frac{\partial v^*}{\partial y^*}=0$. As a consequence, the velocity component v^* is constant in any channel section and is equal to zero at the channel walls, so v^* must be vanishing at any position. The y^*-momentum balance equation can be expressed as $\frac{\partial p^*}{\partial y^*}=0$. Under these hypotheses the governing equations of the present model are[17,22,33]

$$\frac{\partial u^*}{\partial t^*}=-\frac{1}{\rho_{nf}}\frac{\partial P^*}{\partial x^*}+\frac{\mu_{nf}}{\rho_{nf}}\frac{\partial^2 u^*}{\partial y^{*2}}-\frac{\eta}{\rho_{nf}}\frac{\partial^4 u^*}{\partial y^{*4}}-\frac{\sigma_{nf}}{\rho_{nf}}B_0^2u^*+\frac{g(\rho\beta)_{nf}}{\rho_{nf}}(T^*-T_0), \quad \ldots (1)$$

$$\frac{\partial T^*}{\partial t^*}=\frac{k_{nf}}{\left(\rho C_p\right)_{nf}}\frac{\partial^2 T^*}{\partial y^{*2}}+\frac{\mu_{nf}}{\left(\rho C_p\right)_{nf}}\left(\frac{\partial u^*}{\partial y^*}\right)^2+\frac{\eta}{\left(\rho C_p\right)_{nf}}\left(\frac{\partial^2 u^*}{\partial y^{*2}}\right)^2-\frac{1}{\left(\rho C_p\right)_{nf}}\frac{\partial q_r^*}{\partial y^*}+\frac{\sigma_{nf}B_0^{\,2}}{\left(\rho C_p\right)_{nf}}u^{*2}, \quad \ldots (2)$$

Here, x^* axis velocity component is u^*, and $(\rho\beta)_{nf}$, k_{nf}, μ_{nf}, σ_{nf}, $(\rho C_p)_{nf}$, ρ_{nf} characterize the thermal expansion coefficient, thermal conductivity, viscosity, electrical conductivity, heat capacitance, and density of the nanofluid and the relators f, nf, and s symbolize base fluid (ethylene glycol and water (50:50)), nanofluid, and diamond nanoparticles respectively. q_r^* is radiative thermal flux, gravitational acceleration is expressed as g, temperature of the nanofluid is T^*, β is the coefficient of thermal expansion, couple stress viscosity coefficient is η. The appropriate boundary conditions (B.Cs) are

$$\left.\begin{aligned} &at\ y^*=0,\ u^*=0,\frac{\partial^2 u^*}{\partial y^{*2}}=0,T^*=T_0,\\ &at\ y^*=h,\ u^*=0,\frac{\partial^2 u^*}{\partial y^{*2}}=0,T^*=T_1. \end{aligned}\right\} \quad \ldots (3)$$

The thermal characteristics of the mixture (50:50) of ethylene glycol and water (base fluid) and diamond nanoparticles are prearranged in Table 1, and are given as[12,13,15]

$$\rho_{nf}=(1-\phi)\rho_f+\phi\rho_s,\ (\rho C_p)_{nf}=(1-\phi)(\rho C_p)_f+\phi(\rho C_p)_s,$$

$$\mu_{nf}=\frac{\mu_f}{(1-\phi)^{2.5}},\ (\rho\beta)_{nf}=(1-\phi)(\rho\beta)_f+\phi(\rho\beta)_s,$$

$$\frac{k_{nf}}{k_f}=\frac{k_s+2k_f-2\phi(k_f-k_s)}{k_s+2k_f+\phi(k_f-k_s)},\frac{\sigma_{nf}}{\sigma_f}=1+\frac{3(\frac{\sigma_s}{\sigma_f}-1)\phi}{(\frac{\sigma_s}{\sigma_f}+2)-(\frac{\sigma_s}{\sigma_f}-1)\phi}.$$

By implementing the Rosseland assessment for radiative thermal flux (q_r^*) and following[46,47], Eq. (2) becomes,

$$\left(\rho C_p\right)_{nf}\frac{\partial T^*}{\partial t^*}=k_{nf}\frac{\partial^2 T^*}{\partial y^{*2}}+\mu_{nf}\left(\frac{\partial u^*}{\partial y^*}\right)^2+\eta\left(\frac{\partial^2 u^*}{\partial y^{*2}}\right)^2+\frac{16}{3}\frac{\sigma^* T_0^3}{\aleph}\frac{\partial^2 T^*}{\partial y^{*2}}+\sigma_{nf}B_0^{\,2}u^{*2}, \quad \ldots (4)$$

here σ^* is Stephen-Boltzmann constant and $\aleph$ is mean absorption coefficient.

By the aid of ensuing dimensionless variables and parameters,

$$x^*=xh, y^*=yh, t^*=\frac{t}{\omega}, u^*=Uu, P^*=\frac{P\mu_f U}{h}, T^*=T_0+\theta(T_1-T_0), H=\frac{\sqrt{\omega}h}{\sqrt{\nu_f}}, M=B_0h\sqrt{\frac{\sigma_f}{\mu_f}},$$

$$Pr=\frac{\nu_f(\rho C_p)_f}{k_f}, Ec=\frac{U^2}{(C_p)_f(T_1-T_0)}, Re=\frac{Uh}{\nu_f}, Rd=\frac{4\sigma^* T_0^3}{\aleph k_f}, \lambda=\frac{\eta}{\mu_f h^2}, Gr=\frac{g\beta_f(T_1-T_0)h^3}{\nu_f^2}, \quad \ldots (5)$$

Eqns. (1) and (4) become

$$\frac{\partial u}{\partial t}=-\frac{1}{A_1H^2}\frac{\partial P}{\partial x}+\frac{A_2}{A_1}\frac{1}{H^2}\frac{\partial^2 u}{\partial y^2}-\frac{1}{A_1}\frac{\lambda}{H^2}\frac{\partial^4 u}{\partial y^4}-\frac{A_5}{A_1}\frac{M^2}{H^2}u+\frac{A_6}{A_1}\frac{Gr}{H^2Re}\theta, \quad \ldots (6)$$

$$\frac{\partial\theta}{\partial t}=\frac{1}{A_3}\frac{1}{\Pr H^2}\left(A_4+\frac{4}{3}Rd\right)\frac{\partial^2\theta}{\partial y^2}+\frac{A_2}{A_3}\frac{Ec}{H^2}\left(\frac{\partial u}{\partial y}\right)^2+\frac{\lambda}{A_3}\frac{Ec}{H^2}\left(\frac{\partial^2 u}{\partial y^2}\right)^2+\frac{A_5}{A_3}\frac{EcM^2}{H^2}u^2. \quad \ldots (7)$$

Where $A_1=(1-\phi)+\phi\frac{\rho_s}{\rho_f}$, $A_2=\frac{1}{(1-\phi)^{2.5}}$,

$A_3=(1-\phi)+\phi\frac{(\rho C_p)_s}{(\rho C_p)_f}$, $A_4=\frac{k_s+2k_f-2\phi(k_f-k_s)}{k_s+2k_f+\phi(k_f-k_s)}$,

Table 1 — The thermophysical characteristics of diamond nanoparticles and mixture of ethylene glycol and water (50:50)[12-14]

Property	Diamond	Ethylene Glycol and water
$\rho\,(kg/m^3)$	3100	1063.8
$k(W/(mK))$	1000	0.387
$C_p\,(J/(kgK))$	516	3630
$\sigma\,(\Omega m)^{-1}$	1×10^{-14}	9.75×10^{-4}
$\beta\ (1/K)$	1×10^{-4}	5.8×10^{-4}

$$A_5 = 1 + \frac{3\left(\frac{\sigma_s}{\sigma_f} - 1\right)\phi}{\left(\frac{\sigma_s}{\sigma_f} + 2\right) - \left(\frac{\sigma_s}{\sigma_f} - 1\right)\phi},\ A_6 = (1-\phi) + \phi\frac{(\rho\beta)_s}{(\rho\beta)_f},$$

ϕ is nanoparticles volume fraction, Rd is the radiation parameter, M is Hartmann number, λ is couple stress parameter, H is frequency parameter, Re is Reynolds number, Gr is Grashof number, Pr is Prandtl number, and Ec is Eckert number. The B.Cs are

$$\left.\begin{aligned} &at\ y = 0,\ u = 0, \quad \frac{\partial^2 u}{\partial y^2} = 0, \quad \theta = 0, \\ &at\ y = 1,\ u = 0, \quad \frac{\partial^2 u}{\partial y^2} = 0, \quad \theta = 1. \end{aligned}\right\}. \qquad \ldots (8)$$

Solution of the problem

It is presupposed that the current flow is induced by the pulsatile pressure gradient and it is engaged as[33,47]

$$-\frac{\partial P}{\partial x} = \lambda_0 + \varepsilon\lambda_1 e^{it}, \qquad \ldots (9)$$

here, P is the dimensionless fluid pressure, $\varepsilon(<<1)$ is a positive quantity, t is dimentionless time, and λ_0, λ_1 are steady and unsteady magnitudes of pulsatile pressure gradient.

On account of Eq. (9), the solution terms for u and θ can be considered as

$$u = u_0 + \varepsilon u_1 \exp(it), \qquad \ldots (10)$$

$$\theta = \theta_0 + \varepsilon\theta_1 \exp(it), \qquad \ldots (11)$$

Now by substituting Eqs (9)-(11) into the Eqns. (6)-(7), and likening the coefficients of like powers of ε, one can attain

$$A_2\frac{d^2u_0}{dy^2} - \lambda\frac{d^4u_0}{dy^4} - A_5M^2u_0 + \frac{A_6Gr}{Re}\theta_0 + \lambda_0 = 0, \ \ldots (12)$$

$$A_2\frac{d^2u_1}{dy^2} - \lambda\frac{d^4u_1}{dy^4} - A_5M^2u_1 - iA_1H^2u_1 + \frac{A_6Gr}{Re}\theta_1 + \lambda_1 = 0, \ \ldots (13)$$

$$\left(A_4 + \frac{4}{3}Rd\right)\frac{1}{Pr}\frac{d^2\theta_0}{dy^2} + A_2Ec\left(\frac{du_0}{dy}\right)^2 + \lambda Ec\left(\frac{d^2u_0}{dy^2}\right)^2 + A_5M^2Ecu_0^2 = 0, \qquad \ldots (14)$$

$$\left(A_4 + \frac{4}{3}Rd\right)\frac{1}{Pr}\frac{d^2\theta_1}{dy^2} - A_3H^2i\theta_1 + 2A_2Ec\frac{du_0}{dy}\frac{du_1}{dy} + 2\lambda Ec\frac{d^2u_0}{dy^2}\frac{d^2u_1}{dy^2} + 2A_5M^2Ecu_0u_1 = 0. \qquad \ldots (15)$$

The related B.Cs are

$$\left.\begin{aligned} &at\ y = 0,\ u_0 = 0, \quad \frac{d^2u_0}{dy^2} = 0, \quad \theta_0 = 0, u_1 = 0, \quad \frac{d^2u_1}{dy^2} = 0, \quad \theta_1 = 0, \\ &at\ y = 1,\ u_0 = 0, \quad \frac{d^2u_0}{dy^2} = 0, \quad \theta_0 = 1, u_1 = 0, \quad \frac{d^2u_1}{dy^2} = 0, \quad \theta_1 = 0. \end{aligned}\right\} \qquad \ldots (16)$$

An essential physical parameters, the dimensionless shear stress and Nusselt number at the walls are delineated as[33,35,47]

$$\tau = \frac{A_2}{A_1Re}\left(\frac{\partial u}{\partial y}\right)_{y=0,1},\ Nu = \left(A_4 + \frac{4}{3}Rd\right)\left(\frac{\partial\theta}{\partial y}\right)_{y=0,1}. \qquad \ldots (17)$$

Now, the set of Eqs (12) - (15) along with the B. Cs (16) are deciphered numerically by adopting the fourth order Runge-Kutta scheme with the aid of the shooting procedure. The step extent is taken as 0.001, precision is static for the convergence criteria.

Analysis of entropy generation

The entropy generation of the current work in dimensional arrangement is specified as[15,41,44]

$$Ns = \frac{k_{nf}}{T_0^2}\left(1 + \frac{16}{3}\frac{\sigma^*T_0^3}{\aleph k_f}\right)\left(\frac{\partial T^*}{\partial y^*}\right)^2 + \frac{\mu_{nf}}{T_0}\left(\frac{\partial u^*}{\partial y^*}\right)^2 + \frac{\eta}{T_0}\left(\frac{\partial^2 u^*}{\partial y^{*2}}\right)^2 + \frac{\sigma_{nf}B_0^2}{T_0}u^{*2}, \qquad \ldots (18)$$

$$Ns = Nt + Nv + Nj, \qquad \ldots (19)$$

here $Nt = \frac{k_{nf}}{T_0^2}\left(1 + \frac{16}{3}\frac{\sigma^*T_0^3}{\aleph k_f}\right)\left(\frac{\partial T^*}{\partial y^*}\right)^2$, $Nv = \frac{\mu_{nf}}{T_0}\left(\frac{\partial u^*}{\partial y^*}\right)^2 + \frac{\eta}{T_0}\left(\frac{\partial^2 u^*}{\partial y^{*2}}\right)^2$, and $Nj = \frac{\sigma_{nf}B_0^2}{T_0}u^{*2}$ signify heat transmission, couple stress along with dynamical viscosity, and Ohmic heating irreversibilities correspondingly.

The dimensionless arrangement of entropy is

$$NG = A_4\left(1 + \frac{4}{3}Rd\right)\left(\frac{\partial\theta}{\partial y}\right)^2 + \frac{A_2EcPr}{\Omega}\left(\frac{\partial u}{\partial y}\right)^2 + \frac{\lambda EcPr}{\Omega}\left(\frac{\partial^2 u}{\partial y^2}\right)^2 + \frac{A_5M^2EcPr}{\Omega}u^2, \qquad \ldots (20)$$

here $NG = \frac{T_0h^2Ns}{(T_1 - T_0)^2k_f}$ is the characteristic entropy production rate, $\Omega = \frac{T_1 - T_0}{T_0}$ is the temperature variance measuring parameter. On interpretation of Eq. (9), NG can be considered as

$$NG = NG_0 + \varepsilon NG_1e^{it}, \qquad \ldots (21)$$

By embracing the Eqs (10), (11) into the Eq. (21), and relating the coefficients of like powers of ε, one can attain

$$NG_0 = A_4\left(1+\frac{4}{3}Rd\right)\left(\frac{\partial\theta_0}{\partial y}\right)^2+\frac{A_2EcPr}{\Omega}\left(\frac{\partial u_0}{\partial y}\right)^2+\frac{\lambda EcPr}{\Omega}\left(\frac{\partial^2 u_0}{\partial y^2}\right)^2+\frac{A_5M^2EcPr}{\Omega}u_0^2, \quad \ldots (22)$$

$$NG_1 = 2A_4\left(1+\frac{4}{3}Rd\right)\left(\frac{\partial\theta_0}{\partial y}\right)\left(\frac{\partial\theta_1}{\partial y}\right)+\frac{2A_2EcPr}{\Omega}\left(\frac{\partial u_0}{\partial y}\right)\left(\frac{\partial u_1}{\partial y}\right) + \frac{2A_5M^2EcPr}{\Omega}u_0u_1+\frac{2\lambda EcPr}{\Omega}\left(\frac{\partial^2 u_0}{\partial y^2}\right)\left(\frac{\partial^2 u_1}{\partial y^2}\right). \quad \ldots (23)$$

The Bejan number (Be) is elucidated as the ratio between the heat transmission irreversibility and the total entropy (NG), and it is articulated as

$$Be = \frac{A_4\left(1+\frac{4}{3}Rd\right)\left(\frac{\partial\theta}{\partial y}\right)^2}{NG}. \quad \ldots (24)$$

To authenticate the correctness of the current outcomes we done a comparision between the current outcomes and the outcomes secured by NDSolve using MATHEMATICA which are specified in Table 2. It is witnessed that there is a worthy settlement between the current outcomes and the outcomes secured by NDSolve.

Result and Discussion

The current segment is dedicated to interpret the influences of emerging parameters like Hartmann number M, couple stress parameter λ, volume fraction of nanoparticles ϕ, Grashof number Gr, radiation parameter Rd, Eckert number Ec, and frequency parameter H on velocity, temperature, entropy generation, and Bejan number on pulsatile flow of couple stress nanofluid in a vertical channel in Figs. 2-8. In this investigation, u_s, θ_s, NG_s represent steady velocity, steady temperature, and steady entropy of couple stress nanofluid respectively, similarly, u_t, θ_t, NG_t denote the unsteady velocity, unsteady temperature, and unsteady entropy of couple stress nanofluid correspondingly. In the current investigation, the values of emerging non-dimensional parameters are reserved as $\phi = 0.05$, $M = 2$, $\lambda = 0.2$, $\lambda_0 = 1$, $\lambda_1 = 1$, $H = 2$, $Pr = 30.235$, $Ec = 0.6$, $Rd = 1$, $Gr = 4$, $Re = 1$, $\varepsilon = 0.001$, and $t = \pi$ unless otherwise stated.

Table 2 — Comparison between the current outcomes and NDSolve for heat transfer rate at $y = 0$ for the impact of Ec, λ, and Rd when $\phi = 0.05$, $\varepsilon = 0.001$, $M = 2$, $\lambda = 0.2$, $\lambda_0 = 1$, $Rd = 1$, $\lambda_1 = 1$, $H = 2$, $Pr = 30.235$, $Ec = 0.6$, $Gr = 4$, $Re = 1$, and $t = \pi/4$

Parameter	Values	Present results $(Nu)_{y=0}$	NDSolve $(Nu)_{y=0}$
Ec	0.2	3.178957454	3.178959404
	0.4	4.230015605	4.230016469
	0.6	6.434526102	6.434526872
λ	0.5	3.823517457	3.823539358
	1	3.133885685	3.133897986
	1.5	2.914742118	2.914750692
Rd	1	6.434526102	6.434526872
	1.5	6.087884999	6.087887291
	2	6.399236978	6.399237762

Figs 2a-2d interpret the influence of Hartmann number, couple stress parameter, nanoparticles volume fraction, and Grashof number on the steady velocity of the current working fluid. Fig. 2a displays that when the Hartmann number rises it indicates that the magnetic force gains prominence, over the force. As a result the magnetic field exerts an influence on the charged nanoparticles in the nanofluid. This causes deviation of the charged nanoparticles due to the field ultimately resulting in alterations to the flow pattern of the fluid. In scenarios there may be a decrease in velocity of the nanofluid due, to heightened resistance caused by this intensified force. Fig. 2b illustrates that the inclusion of nanoparticles, in the nanofluid can cause a Newtonian response because of the interactions between particles and the base fluid at the nanoscale. When combined with the influence of couple stress it is possible for the nanofluid to show a decrease in viscosity. Fig. 2c elucidates that the velocity is a dwindling function of nanoparticles volume fraction. The cause behind this is the intensification in nanoparticles volume fraction level up the density of the couple stress nanofluid hence there is a fall in the velocity. The velocity of current working nanofluid is increasing for the higher values of Grashof number, this increase is due to the effectiveness of the buoyant force contradicting the gravitational acceleration, which is plotted in Fig. 2d.

The effects of applied magnetic field, couple stress parameter, nanoparticles volume fraction, and the frequency parameter on unsteady velocity for various values are delineated in Figs 3a-3d. Enhancing the effect of applied magnetic field, declining the velocity, for the reason that the delaying forces caused

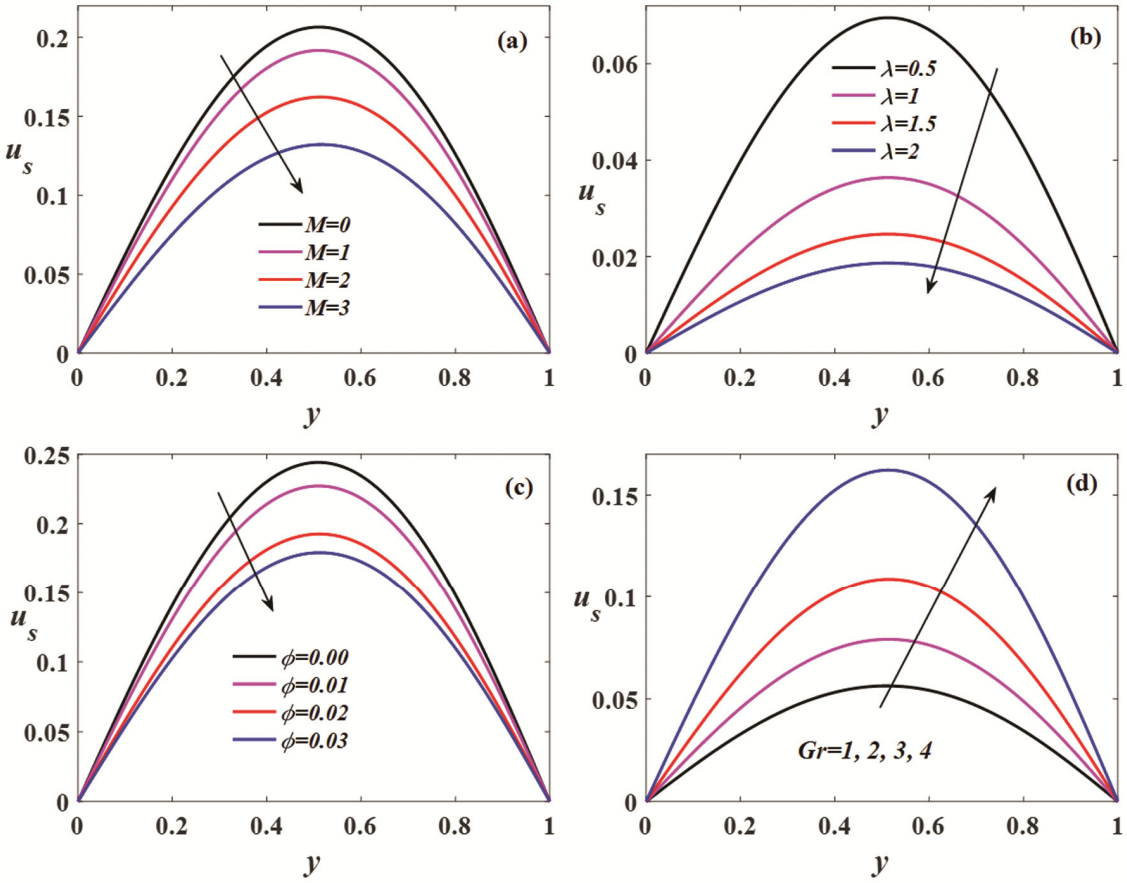

Fig. 2 — (a) influence of M =0, 1, 2, 3, (b) influence of λ =0.5, 1, 1.5, 2, (c) influence of ϕ = 0.00, 0.01, 0.02, 0.03, (d) influence of Gr = 1, 2, 3, 4 on steady velocity distribution

by the applied magnetic field act normal to track of the current flow, which is portrayed in Fig. 3a. Fig. 3b shows the amplifying the couple stress viscosity intensifying the density of the current working nanofluid which leads the dwindle nature in velocity. The same behaviour is true for intensifying nanoparticles volume fraction, because the increment in the density of the current working fluid slows down the movement of the couple stress nanofluid, which is displayed in Fig. 3c. The influence of frequency parameter on unsteady velocity is portrayed in Fig. 3d. From the Figs. 3a-3d, one can infer that the high velocity is in the vicinity of the centre of the channel.

The impressions of Eckert number, Hartmann number, couple stress viscosity, thermal radiation, nanoparticles volume fraction, and Grashof number on steady temperature of couple stress nanofluid are presented in Figs 4a-4f. Fig. 4a shows that elevating Eckert number uplifting the temperature of couple stress nanofluid, for the reason that growing Eckert number dissipating additional heat into the system from the frictional heating which helps to improve the temperature. Fig. 4b displays that the enhancement in the effect of Hartmann number dwindling the temperature, for the reason that suspending forces fashioned by the applied magnetic field act upright to the flow path of the current working fluid which makes the flow slow down. Fig. 4c demonstrates the impression of couple stress parameter on the steady temperature, which states that intensifying couple stress viscosity dwindling the flow of the nanofluid which is not encouraging the temperature. From Fig. 4d, one can infer that intensifying the thermal radiation decreasing the temperature, for the reason that the radiation parameter corresponds to the thermal dispersion of heat conductivity. Fig. 4e elucidates that increasing nanoparticles volume fraction encouraging the thermal absorption, due to the good heat conductive coefficient transfer the maximum heat hence there is a fall in the temperature of current working nanofluid. Unlike the Fig. 4e,

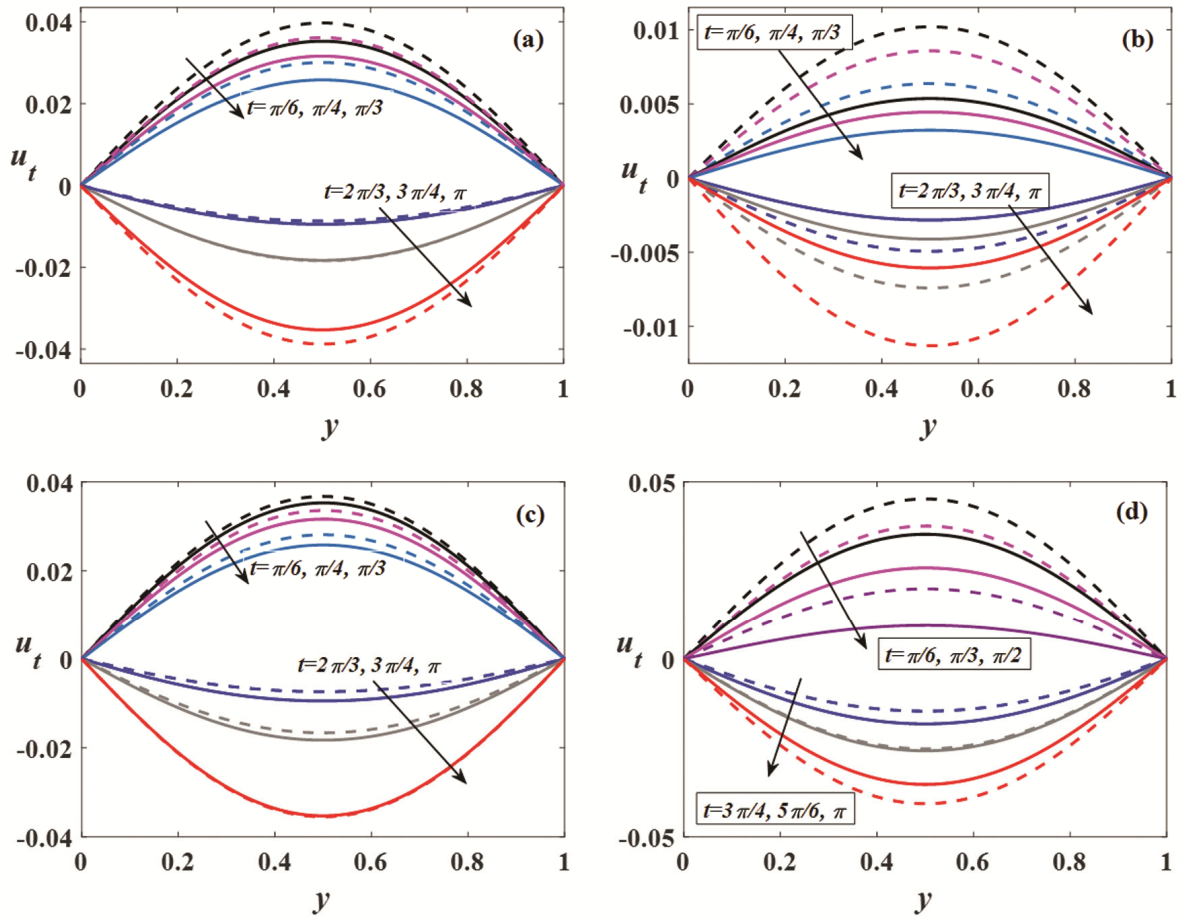

Fig. 3 — (a) Effect of M and $t = \frac{\pi}{6}, \frac{\pi}{4}, \frac{\pi}{3}, \frac{2\pi}{3}, \frac{3\pi}{4}, \pi$, dashed line $M = 0$, solid line $M = 2$, (b) impact of λ and $t = \frac{\pi}{6}, \frac{\pi}{4}, \frac{\pi}{3}, \frac{2\pi}{3}, \frac{3\pi}{4}, \pi$, dashed line λ =1, solid line λ =2,(c) impact of ϕ and $t = \frac{\pi}{6}, \frac{\pi}{4}, \frac{\pi}{3}, \frac{2\pi}{3}, \frac{3\pi}{4}, \pi$,, dashed line ϕ = 0.00, solid line ϕ =0.05, (d) impact of H and $t = \frac{\pi}{6}, \frac{\pi}{3}, \frac{\pi}{2}, \frac{3\pi}{4}, \frac{5\pi}{6}, \pi$, dashed line H =1, solid line H= 2, on unsteady velocity distribution

there is an opposite behaviour in the temperature of current working nanofluid can be found for the increasing values of Grashof number, which is delineated in Fig. 4f.

The impressions of Eckert number, radiation parameter, volume fraction of nanoparticles, and the frequency parameter on the unsteady temperature are demonstrated in Figs 5a-5d. Fig. 5a illustrates that the temperature is increasing for magnifying viscous dissipation, which is due to the enhancement in Eckert number dissipating additional energy in the system. The opposite trend can be seen in the temperature profiles from Fig. 5a, for enhancing radiative thermal flux, which is plotted in Fig. 5b. The similar trend as Fig. 5b, can be found in the temperature of working nanofluid for the uplifting nanoparticles volume fraction which is presented in Fig. 5c. Fig. 5d elucidates that increasing frequency parameter encouraging the temperature, because the enhancement in frequency boosts up the temperature. From the Figs 5a-5d, it is clear that the maximum temperature is in the vicinity of the centre of the channel.

Figs 6a-6f elucidate the sway of Eckert number, Hartmann number, couple stress viscosity, thermal radiation, nanoparticles volume fraction, and Grashof number on the steady entropy of couple stress nanofluid. Fig. 6a displays the impact of viscous dissipation on the entropy, which states that magnifying viscous dissipation producing extra heat due to the frictional heating which aids to lift up the

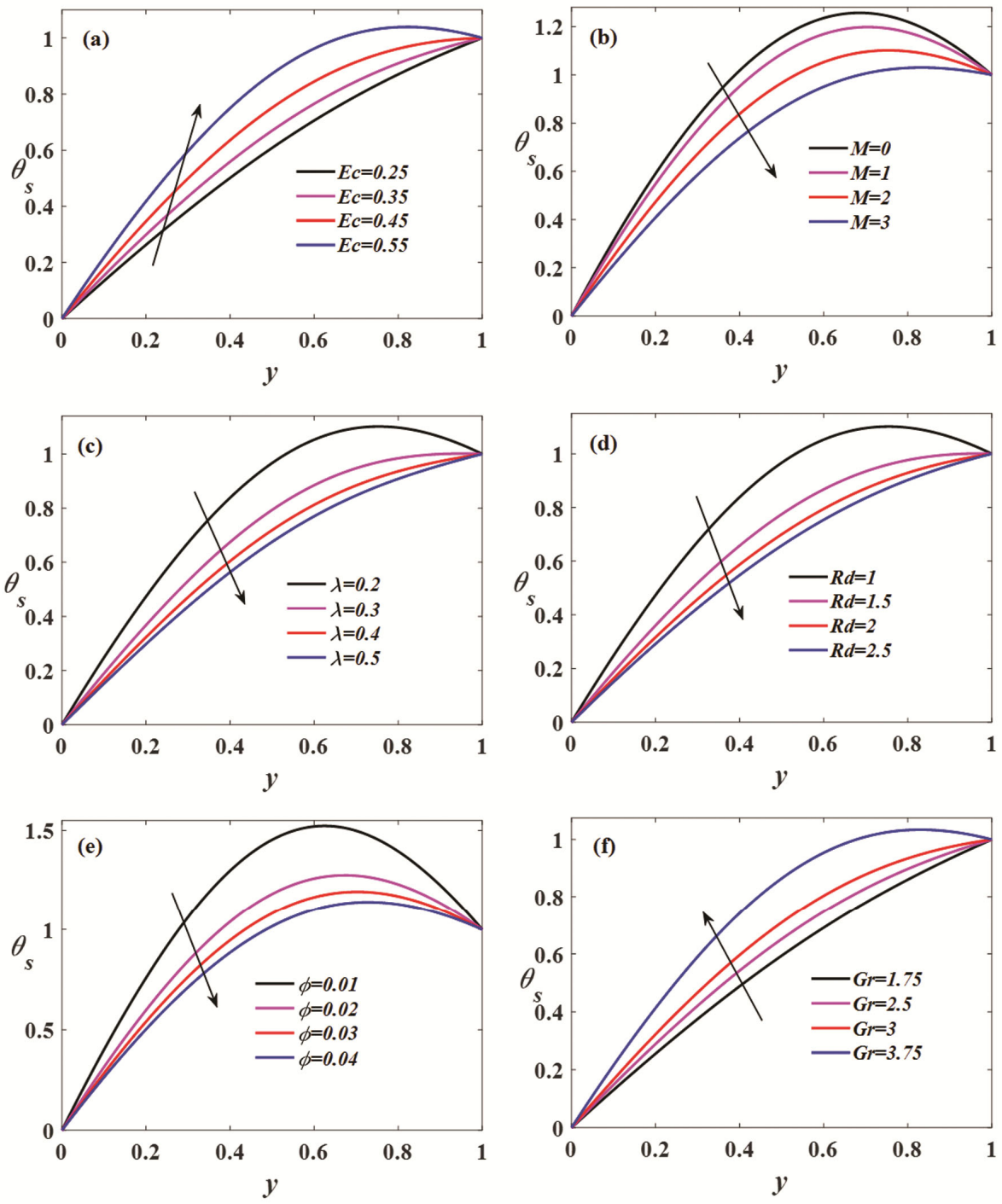

Fig. 4 — (a) Impression of Ec = 0.25, 0.35, 0.45, 0.55, on θ_s, (b) impression of M = 0, 1, 2, 3, on θ_s, (c) impression of λ = 0.2, 0.3, 0.4, 0.5, on θ_s, (d) impression of Rd = 1, 1.5, 2, 2.5, on θ_s, (e) impression of ϕ =0.01, 0.02, 0.03, 0.04, on θ_s, (f) impression of Gr = 1.75, 2.5, 3, 3.75, on θ_s

entropy of the current working fluid. Fig. 6b presents the effect of Hartmann number decreasing the entropy for the reason that the suspending forces caused by the applied magnetic field slow down the flow which corresponds to reduce the energy transmission. The similar behaviour can be seen in entropy for augmenting couple stress parameter, which is presented in Fig. 6c, because the increment in the

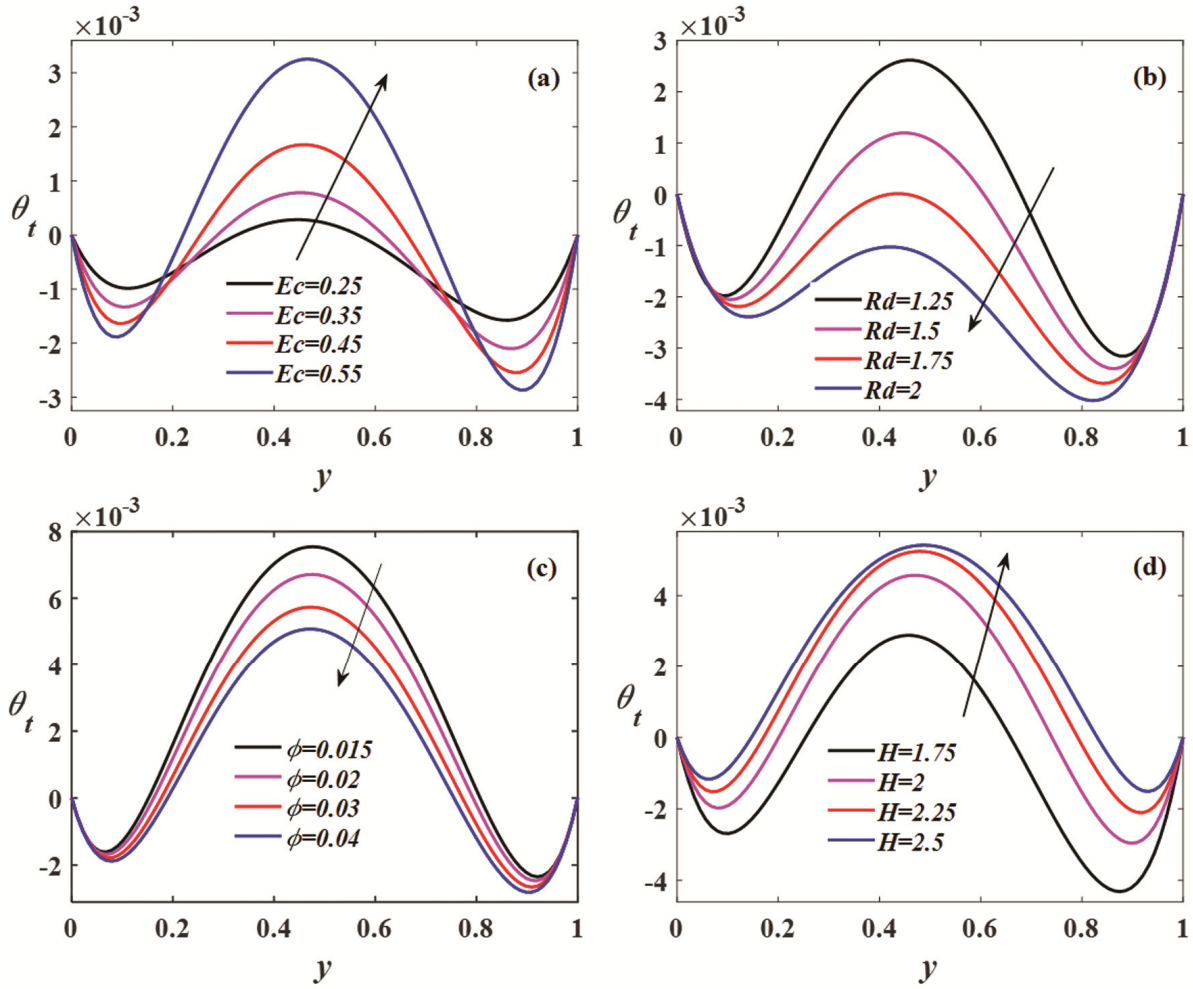

Fig. 5 — (a) Influence of Ec = 0.25, 0.35, 0.45, 0.55, on θ_t, (b) influence of Rd = 1.25, 1.5, 1.75, 2, on θ_t, (c) influence of ϕ=0.015, 0.02, 0.03, 0.04, on θ_t, (d) influence of H=1.75, 2, 2.25, 2.5, on θ_t

couple stress viscosity decreasing the temperature of nanofluid. Fig. 6d elucidates that rising the effect of thermal radiation encouraging the entropy of the couple stress nanofluid, due to the thermal radiation's relative commitment with the conductive heat. Unlike the Fig. 6d, entropy of couple stress nanofluid is decelerating for intensifying nanoparticles volume fraction, which is presented in Fig. 6e. Fig. 6f shows the influence of Grashof number on entropy, which states that enhancing Grashof number boosting the entropy of the current working system due to the Grashof number is encouraging the temperature of couple stress nanofluid.

The influences of Eckert number, Hartmann number, couple stress parameter, and nanoparticles volume fraction on the unsteady entropy are presented in Figs 7a-7d. Fig. 7a portrays that enhancement in Eckert number encouraging the entropy, because the Eckert number's commitment with the additional energy dissipation.When the Eckert number goes up it can cause alterations, in the entropy of the fluid. Entropy is a way to measure the level of disorder or randomness in a system. When the Eckert number increases the flow of fluid becomes more energetic which lead to changes in temperature and pressure within the nanofluid. These changes, in temperature and pressure can affect the entropy of the fluid. Fig. 7b illustrates the amplifying Hartmann number dwindling the entropy of the current system, for the reason that the suspending forces produced by the applied magnetic field makes the flow slow down. The same behaviour as Fig. 7b, can be found in the entropy of the current system for the

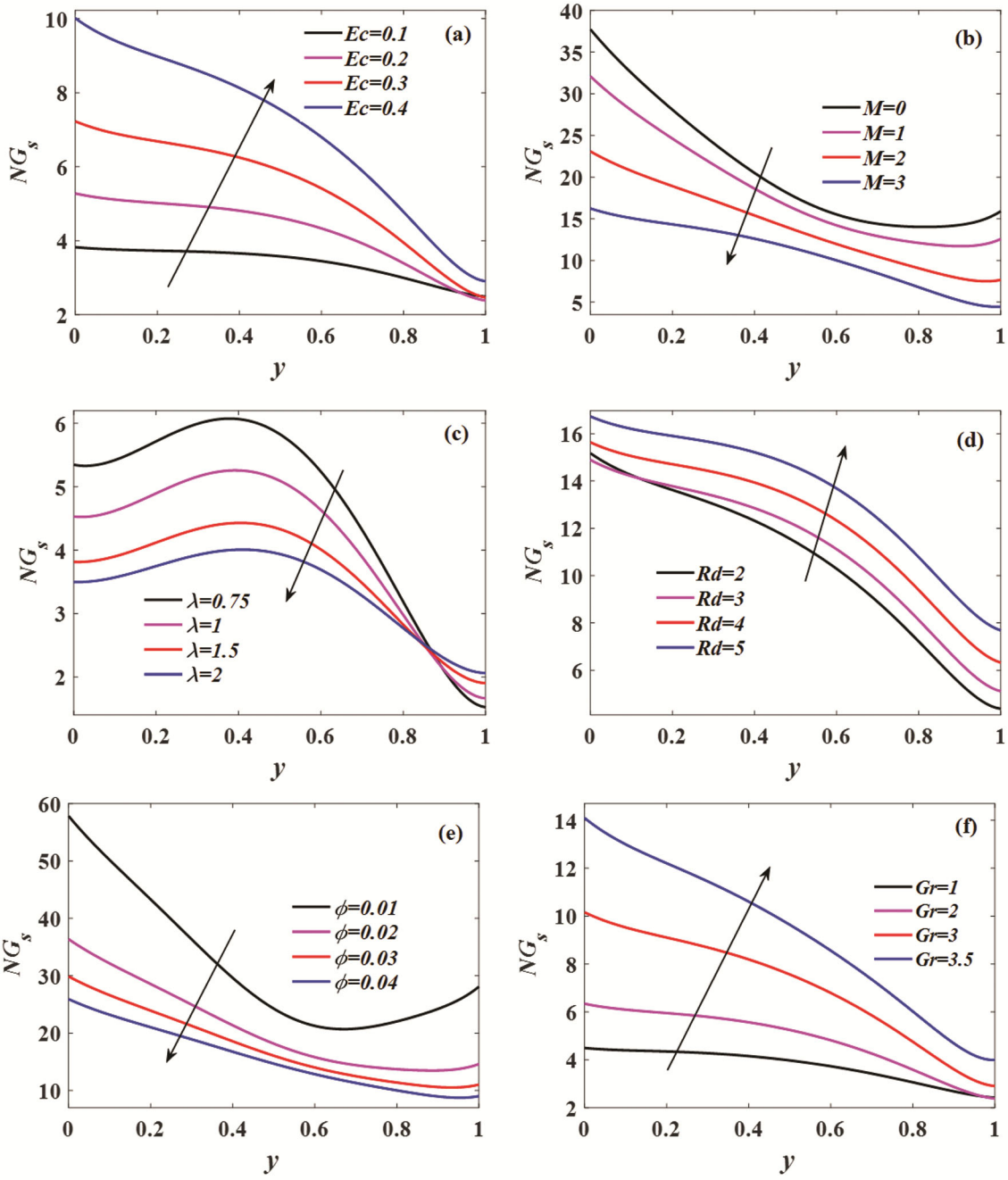

Fig. 6 — (a) Impression of Ec = 0.1, 0.2, 0.3, 0.4, on NG_s, (b) impression of M = 0, 1, 2, 3, on NG_s, (c) impression of λ =0.75, 1, 1.5, 2, on NG_s, (d) impression of Rd = 2, 3, 4, 5, on NG_s, (e) impression of ϕ =0.01, 0.02, 0.03, 0.04, on NG_s, (f) impression of Gr = 1, 2, 3, 3.5, on NG_s

augmenting couple stress viscosity, and the volume fraction of nanoparticles, which are drawn in Figs. 7c-7d. The maximum entropy can be identified in the centre of the channel, which can be noticed in Figs 7a-7d.

Figs 8a-8d are drawn to infer the impacts of viscous dissipation, couple stress viscosity, radiation parameter, and the volume fraction of nanoparticles on the Bejan number of the couple stress nanofluid. Fig. 8a displays the acceleration in viscous dissipation results the deceleration in the Bejan number. Fig. 8b shows the impact of couple stress parameter on the Bejan number of the current model, which elucidates that increasing

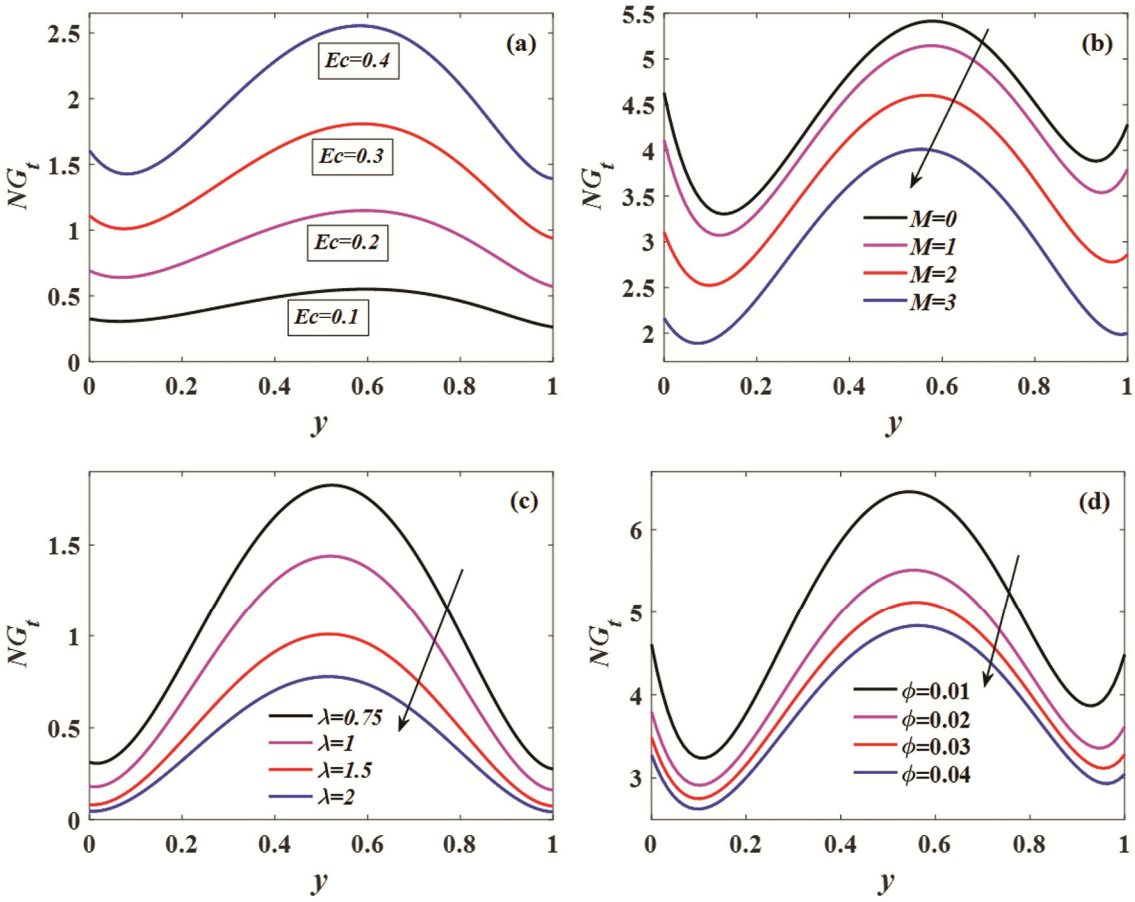

Fig. 7 — (a) Influence of *Ec* = 0.1, 0.2, 0.3, 0.4, on NG_t, (b) influence of *M* = 0, 1, 2, 3, on NG_t, (c) influence of λ =0.75, 1, 1.5, 2, on NG_t, (d) influence of ϕ =0.01, 0.02, 0.03, 0.04, on NG_t

couple stress viscosity boosting up the Bejan number. Fig. 8c presents that the enhancing thermal radiation increasing the Bejan number of the current system. The impact of the nanoparticles volume fraction on the Bejan number is plotted in Fig. 8dwhich shows that when nanoparticles are present, in amounts the nanofluid tends to exhibit improved conductivity and in certain instances changes in viscosity compared to the pure base fluid. This can result in heat transfer within the nanofluid. Consequently the Bejan number may decrease as heat transfer becomes relative, to viscous dissipation. This figure indicates that the Bejan number is falling for magnifying nanoparticles volume fraction.

The influences of viscous dissipation, couple stress parameter, volume fraction of nanoparticles, radiation parameter, and Hartmann number on the steady and unsteady shear stress distributions $\tau_s\left(\left(A_2/(A_1Re)\right)u_0'\right)$ and $\tau_t\left(\left(A_2/(A_1Re)\right)\varepsilon u_1'\exp(it)\right)$ at the walls $y=0$ and $y=1$ are prearranged in Table 3. From this table, it is clear that the steady and unsteady shear stresses are increased for enhancing Eckert number at $y=0$ whereas the reverse is true at $y=1$. The increment in couple stress parameter, thermal radiation, Hartmann number and nanoparticles volume fraction is reducing the shear stress at $y=0$ and it is enhancing the shear stress at $y=1$. The influences of viscous dissipation, couple stress parameter, volume fraction of nanoparticles, radiation parameter, and Hartmann number on the steady and unsteady heat transmission distributions $Nu_s\left(\left(A_4+(4/3)Rd\right)\theta_0'\right)$ and $Nu_t\left(\left(A_4+(4/3)Rd\right)\varepsilon\theta_1'\exp(it)\right)$ at the walls $y=0$ and $y=1$ are prearranged in Table 4. From this table, it is clear that the steady and unsteady heat trasfer rates are reduced for intensifying couple stress

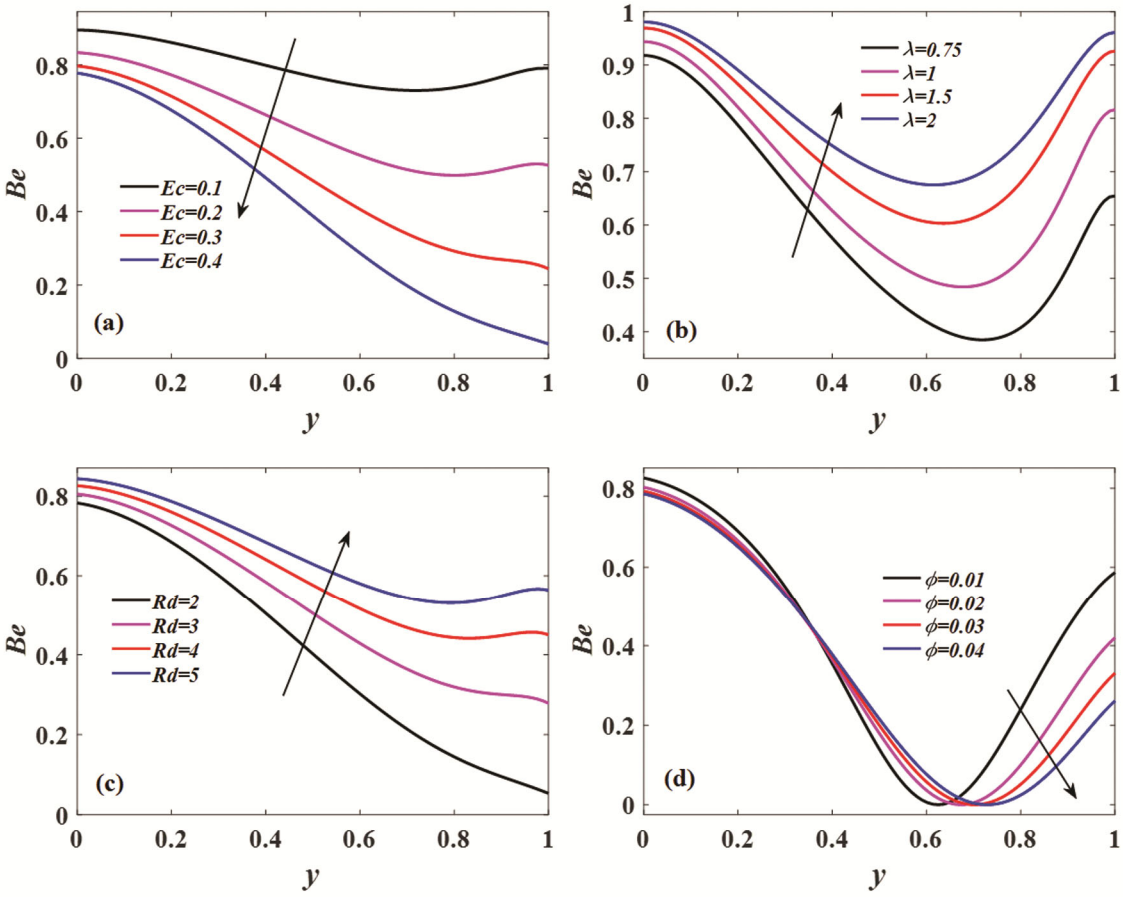

Fig. 8 — (a) Effect of *Ec* = 0.1, 0.2, 0.3, 0.4, on *Be*, (b) effect of λ = 0.75, 1, 1.5, 2, on *Be*, (c) effect of *Rd* = 2, 3, 4, 5, on *Be*, (d) effect of ϕ =0.01, 0.02, 0.03, 0.04, on *Be*

Table 3 — Shear stress distributions for the influence of Ec, λ, ϕ, Rd, and M at, $\varepsilon = 0.1$, $\lambda = 0.2$, $H = 2$, $\lambda_0 = 1$, $\lambda_1 = 1$, $\Pr = 30.235$, $M = 2$, $Re = 1$, $Rd = 1$, $Ec = 0.6$, $Gr = 4$, $t = \pi/4$

Parameter	values	at $y = 0$		at $y = 1$	
		τ_s	τ_t	τ_s	τ_t
Ec	0.1	0.354073	0.353176	-0.009763	-0.009796
	0.2	0.370758	0.370522	-0.009919	-0.009927
	0.3	0.391181	0.390932	-0.010059	-0.010067
λ	0.5	0.220246	0.220184	-0.005283	-0.005287
	1	0.115292	0.115260	-0.002850	-0.002852
	1.5	0.078218	0.078169	-0.001947	-0.001948
ϕ	0.01	0.724985	0.724524	-0.011091	-0.011100
	0.02	0.612535	0.612146	-0.010900	-0.010909
	0.03	0.568925	0.568564	-0.010785	-0.010794
Rd	1	0.514227	0.513900	-0.010586	-0.010595
	1.25	0.467765	0.467467	-0.010549	-0.010558
	1.5	0.442639	0.442357	-0.010535	-0.010544
M	0	0.658529	0.658110	-0.012063	-0.012073
	1	0.610379	0.609991	-0.011652	-0.011661
	2	0.514227	0.513900	-0.010586	-0.010595

Table 4 — Distributions of steady and unsteady heat transfer rate for the influence of Ec, λ, ϕ, Rd, and M at, $\varepsilon = 0.1$, $H = 2$, $\lambda = 0.2$, $\lambda_0 = 1$, $\Pr = 30.235$, $\lambda_1 = 1$, $M = 2$, $Re = 1$, $Rd = 1$, $Ec = 0.6$, $Gr = 4$, $t = \pi/4$

Parameter	values	at $y = 0$		at $y = 1$	
		Nu_s	Nu_t	Nu_s	Nu_t
Ec	0.1	2.805044	2.795930	0.005086	0.005639
	0.2	3.178862	3.168882	0.011084	0.011678
	0.3	3.638145	3.621480	0.017290	0.018237
λ	0.5	3.823389	3.816344	0.015291	0.015820
	1	3.133828	3.131896	0.007237	0.007379
	1.5	2.914705	2.913367	0.004710	0.004772
ϕ	0.01	10.473752	10.365405	0.052994	0.056465
	0.02	8.187057	8.108393	0.047007	0.049966
	0.03	7.375805	7.307087	0.044820	0.047591
Rd	1	6.434144	6.376550	0.042183	0.044729
	1.25	6.092697	6.045040	0.042939	0.045269
	1.5	6.087490	6.044816	0.044725	0.046942
M	0	8.220668	8.126227	0.054728	0.058381
	1	7.571105	7.489967	0.050652	0.053939
	2	6.434144	6.376550	0.042183	0.044729

viscosity, and nanoparticles volume fraction whereas the reverse trend can be seen for magnifying viscous dissipation at the channel walls. A rise in thermal radiation increasing the heat transfer rate at the right wall while the reverse is true at the left wall.

Conclusion

The current work discloses the entropy generation of oscillating hydromagnetic couple stress nanofluid flow between a pair of vertical parallel walls. The impacts of Ohmic heating, viscous dissipation, and thermal radiation are taken into the consideration. The current inspection is noteworthy in nano-drug transportation, complex and biological fluids, drug targeting, solar energy, tissue heat conduction, and pharmacheuticals. The numerical upshots for emerging parameters are deliberated by employing the fourth order Runge-Kutta process cum shooting procedure. The major results of the present investigation are shortened here:

(i) An escalating Grashof number encouraging the velocity and the reverse is true with increasing couple stress viscosity, nanoparticles' volume fraction, and Hartmann number.

(ii) The increment in couple stress viscosity declines the temperature whereas the reverse behavior can be found with intensifying viscous dissipation.

(iii) An increment in Hartmann number, couple stress parameter, thermal radiation, and nanoparticles' volume fraction decreases the temperature and the reverse is true with a increment in Grashof number.

(iv) The shear stress is decelerating with the boost up in Hartmann number, and couple stress parameter at left wall while it is accelerating with the increment in viscous dissipation at the left wall.

(v) The rate of heat transfer is decelerating with the boost up in Hartmann number while it is accelerating with the increment in viscous dissipation.

(vi) Entropy is escalating for intensifying viscous dissipation, and thermal radiation and the reverse is true with a increment in nanoparticles' volume fraction, Hartmann number, and couple stress parameter. Bejan number is dwindling for escalating volume fraction of nanoparticles, and viscous dissipation while it is enhancing with the escalation in couple stress parameter, and thermal radiation.

The application of a magnetic field, as well as the nanoparticle volume fraction, play critical roles in controlling the heat transfer rate of couple stress nanofluids. Optimizing these characteristics can result in better heat transfer performance, making nanofluids appealing candidates for a wide range of technical applications, including heat exchangers, electronic cooling systems, and advanced thermal management technologies. Furthermore, the present work can be explored in various geometries for the advancement of diverse applications.

Nomenclature

C_p specific heat
Ec Eckert number
Gr Grashof number
h distance between the plates
k_f thermal conductivity of the base fluid
k_s thermal conductivity nanoparticles
k_{nf} thermal conductivity of nanofluid
M Hartmann number
NG characteristic entropy production rate
P^* pressure
Pr Prandtl number
q_r radiative heat flux
Rd radiation parameter
T^* temperature of the nanofluid
t^* time
u^* velocity component in x^* - direction

Greek letters

ε positive quantity ($<<1$)
η coefficient of couple stress viscosity
λ couple stress parameter
μ_f viscosity of the base fluid
μ_{nf} dynamic viscosity of the nanofluid
ρ_f density of the base fluid
ρ_s density of nanoparticles
ρ_{nf} density of nanofluid
$(\rho C_p)_f$ heat capacitance of the base fluid
$(\rho C_p)_s$ heat capacitance of nanoparticles
$(\rho C_p)_{nf}$ effective specific heat of nanofluid
σ_f electrical conductivity of the base fluid
σ_s electrical conductivity of nanoparticles
σ_{nf} electrical conductivity of the nanofluid
ϕ nanoparticle volume fraction

References

1 Choi S U S & Eastman J A, *Am Soc Mech Eng Fluids Eng Div FED*, 231 (1995) 99.
2 Hatami M, Hatami J & Ganji D D, *Comput Methods Programs Biomed*, 113 (2014) 632.
3 Hayat T, Shah F & Alsaedi A, *Int Commun Heat Mass Transf*, 111 (2020) 104454.
4 Mandal S & Shit G, *Chinese J Phys*, 74 (2021) 239.
5 Monaledi R L & Makinde O D, *Defect Diffus Forum*, 387 (2018) 273.
6 Okonkwo EC, Wole-Osho I, Almanassra I W, Abdullatif Y M & Al-Ansari T, *J Therm Anal Calorim*, 145 (2021) 2817.
7 Rikitu B H, Makinde O D & Enyadene L G, *J Nanofluids*, 10 (2021) 31.
8 Sheikholeslami M, Ganji D D, Li Z & Hosseinnejad R, *Sci Iran*, 26 (2019) 1405.
9 Rajamani S, Reddy A S, Srinivas S & Ramamohan T R, *Indian J Pure Appl Phys*, 60 (2022) 354.
10 Santosh Chaudhary, *Indian J Chem Technol*, 29 (2022) 311.
11 Azimi M, Ganji D D, Azimi A & Riazi R, *Indian J Chem Technol*, 25 (2018) 231.
12 Basha H T, Sivaraj R, Reddy A S & Chamkha A J, *Eur Phys J Spec Top*, 228 (2019) 2531.
13 Hosseinzadeh K, Asadi A, Mogharrebi A R, Azari M E & Ganji D D, *J Therm Anal Calorim*, 143 (2021) 1081.
14 Massoudi M D & Hamida M B B, *Eur Phys J Plus*, 135 (2020) 11.
15 Saleh B & Sundar L S, *Powder Technol*, 380 (2021) 430.
16 Muneeshwaran M, Srinivasan G, Muthukumar P & Wang C C, *Int Commun Heat Mass Transf*, 125 (2021) 105341.
17 Devakar M & Iyengar T K V, *Nonlinear Anal Model Control*, 15 (2010) 29.
18 Govindarajulu K & Reddy A S, *Proc Inst Mech Eng Part E J Process Mech Eng*, 236 (2022) 1544.
19 Hayat T, Muhammad T & Alsaedi A, *Chinese J Phys*, 55 (2017) 930.
20 Rajkumar D & Reddy A S, *Phys Scr*, 96 (2021) 125233.
21 Sithole H, Mondal H, Goqo S, Sibanda P & Motsa S, *Appl Math Comput*, 339 (2018) 820.
22 Stokes V K, *Phys Fluids*, 11 (1968) 1131.
23 Adesanya S O & Makinde O D, *Comput Appl Math*, 34 (2015) 293.
24 Ramesh K, Reddy M G & Souayeh B, *Appl Math Mech (English Ed)*, 42 (2021) 593.
25 Dhlamini M, Mondal H, Sibanda P & Motsa S, *Int J Appl Comput Math*, 7 (2021) 2.
26 Umavathi J C & Bég O A, *Microfluid Nanofluidics*, 25 (2021) 1.
27 Usman M, Gul T, Khan A, Alsubie A & Ullah M Z, *Int Commun Heat Mass Transf*, 127 (2021) 105562.
28 Rajamani S & Reddy A S, *Proc Inst Mech Eng Part E J Process Mech Eng*, 235 (2021) 1895.
29 Jawad M, Khan A & Shah S, *Brazilian J Phys*, 51 (2021) 1096.
30 Datta N, Dalal D C & Mishra S K, *Int J Heat Mass Transf*, 36 (1993) 1783.
31 Esfe M H, Bahiraei M, Torabi A, & Valadkhani M, *Int Commun Heat Mass Transf*, 120 (2021) 104859.
32 Malathy T & Srinivas S, *Int Commun Heat Mass Transf*, 35 (2008) 681.
33 Radhakrishnamacharya G & Maiti M K, *J Heat Mass Transf*, 20 (1977) 171.
34 Wang C Y, *J Appl Mech*, *Trans ASME*, 38 (1971) 553.
35 Zamzari F, Mehrez Z, El Cafsi A, Belghith A & Le Quéré P, *J Hydrodyn*, 29 (2017) 632.
36 Srinivas S, Kumar C K & Reddy A S, *Nonlinear Anal Model Control*, 23 (2018) 213.
37 Shawky H M, *Heat Mass Transf*, 45 (2009) 1261.
38 Ahmed S & Xu H, *Int. Commun. Heat Mass Transf*, 120 (2021) 105042.
39 Ye Q, Zhang Y & Wei J, *Appl Therm Eng*, 196 (2021) 117275.
40 Venkatesan G & Reddy A S, *Eur Phys J Spec Top*, 230 (2021) 1475.
41 Bejan A, *J Heat Transfer*, 101 (1979) 718.
42 Dhahri H, Slimi K & Nasrallah S B, *J Porous Media*,11 (2008) 557.
43 Hosseinzadeh K, Mardani M R, Salehi S, Paikar M, Waqas M & Ganji D D, *Pramana - J Phys*, 95 (2021) 57.
44 Upadhya S M, Raju S V S R, Raju C S K, Shah N A & Jae D C, *Chinese J Phys*, 77 (2021) 1080.
45 Govindarajulu K & Reddy A S, *Phys Fluids*, 34 (2022) 013105.
46 Kumar M A, Reddy Y D, Rao V S & Goud B S, *Case Stud Therm Eng*, 24 (2021) 100826.
47 Kumar C K, Srinivas S & Reddy A S, *J Mech*, 36 (2020) 535.
48 Zhao T, Khan M R, Chu Y, Issakhov A, Ali R & Khan S, *Appl Math Mech (English Ed)*, 42 (2021) 1205.
49 Loganathan K, Mohana K, Mohanraj M, Sakthivel P & Rajan S, *J Therm Anal Calorim*, 144 (2021) 1935.